Techniques

Methods for Study of Raindrop Impact on Plant Surfaces with Application to Predicting Inoculum Dispersal by Rain

K. M. Reynolds, L. V. Madden, D. L. Reichard, and M. A. Ellis

First, second, and fourth authors: postdoctoral research associate, and associate professors, Department of Plant Pathology, Ohio State University (OSU), Ohio Agricultural Research and Development Center (OARDC); third author: agricultural engineer, Agricultural Research Service, USDA, Wooster 44691.

Salaries and research support provided by state and federal funds (especially USDA Competitive Grant 85-CRCR-1-1537) appropriated to OARDC-OSU, Journal Article 37-86.

Use of trade names implies neither endorsement of products by OARDC or USDA nor criticism of similar ones not mentioned.

We thank D. Collins for his assistance and R. Alvey and P. Keck for their assistance in developing the timing circuitry and strobe system.

Accepted for publication 9 July 1986 (submitted for electronic processing).

ABSTRACT

Reynolds, K. M., Madden, L. V., Reichard, D. L., and Ellis, M. A. 1987. Methods for study of raindrop impact on plant surfaces with application to predicting inoculum dispersal by rain. Phytopathology 77:226-232.

A drop-generating and photographic system has been developed to obtain detailed information on splash dispersal events. Uniform drops 0.18–1.89 mm in diameter are produced by a piezoelectric crystal that is activate a microprocessor-controlled timing circuit that can trigger up to mm are produced by a solenoid pump. Both drop generators can produce single drops on demand. The drop generator activation signal is used to activate a microprocessor-controlled timing circuit that can trigger-up seven strobe lamps for use in multiple-exposure photography. A primary, programmable delay is used to control the start of the flash sequence. Delay between flashes is controlled by the frequency of an oscillator signal input to the timer. Strobe sequences can be used to determine the velocity, size, and number of droplets formed by a splash crown.

The importance of rain impact as a mechanism for the liberation and dispersal of inoculum of many fungal and bacterial plant pathogens has been recognized since the early pioneering work of Faulwetter (4,5) and Stepanov (30). Effective dispersal of plant pathogens by rain splash has been shown to occur in the absence of wind (4–9,11–13,28,29,31). Most studies of splash dispersal have focused on the role of rain impact in inoculum liberation and on descriptions of dispersal and infection gradients that result from splash dispersal (10). Several studies indicate that in the absence of insects that can serve as agents of dispersal, rain splash is a virtual requirement for successful liberation of some fungal spores or bacterial cells (11,17,27). In such systems, wind may augment dispersal, but it cannot initiate the process. Even for propagules that are characteristically liberated by dry wind, liberation by impact of raindrops or drip from the canopy may become a requirement when inoculum is held in a surface film of water (27).

The publication costs of this article were defrayed in part by page charge payment. This article must therefore be hereby marked "*advertisement*" in accordance with 18 U.S.C. § 1734 solely to indicate this fact.

Characteristics of the inoculum-bearing surface that affect dispersal, such as the presence of moisture, rigidity, and angle of inclination, have been investigated (11,28). However, detailed information on the entrainment of inoculum in splash droplets that are produced by impacting raindrops is lacking. This lack of information is due, in part, to the difficulties of producing individual drop impact events. A greater depth of understanding of the mechanics of splash dispersal would be possible if the events of a single drop impact were more completely understood. A further limitation of previous methods that have been used to study splash phenomena has been the drop delivery system. The standard technique for generating drops has involved the use of syringe needles that depend on gravity feed. Only drops larger than 2 mm in diameter can be produced by this type of drop generator. Large drops constitute a small fraction of incident raindrops (3,19,21). Eighty percent of drops in a 5-mm·hr^{-1} shower, for example, have a diameter $<$ 1 mm, and drops with diameters $>$ 3 mm are quite rare (21). Small drops have been produced with an aspirated syringe system, but it requires the production of a drop stream (14).

A device that could produce single drops of uniform size on demand would facilitate the type of detailed study that is necessary. Such drop generators can be fabricated using a piezoelectric crystal to dispense the drops. Reichard et al (25) used a model 3050 droplet generator (TSI Inc., St. Paul, MN) containing a piezoelectric crystal to produce streams of small-diameter drops of uniform size for use in the study of spray drop impact on foliage.

The present study describes modifications to the drop production methods of Reichard et al (25) that allow production on demand of single drops of desired size that represent the entire raindrop spectrum. High-speed cinematography has frequently been used to study the behavior of falling drops or drop impact (15,16,20). The cinematographic technique has proven to be extremely valuable because details of a single event can be recorded in great detail. However, a distinct disadvantage of cinematography is the relatively high cost of recording a single event. Consequently, methods for multiple exposure, high-speed still photography of individual drop impact events, employing microprocessor-controlled strobe lamps, are also described. These new methods facilitate the simultaneous determination of drop number, drop size, and drop velocity.

MATERIALS AND METHODS

Production of single, uniform drops. Drops with diameters of 0.18–1.89 mm were produced with a drop generator containing a piezoelectric crystal (model 60690 PZT unimorph, Vernitron Piezoelectric Division, Cleveland, OH) (Fig. 1A). Piezoelectric crystals are electromechanical transducers that are deformed when a current is applied across their surface (1) and have been used in applications such as ultrasonic cleaners and ink-jet printers (1). The generator was similar in design to generators used for ink-jet printers and generators made by Young (32) at ICI and Qian et al (23). The outlet of the chamber that houses the crystal was machined to a Luer taper (five degrees) to accept Luer-lok needles. Plastic needle covers with a Luer taper, to which electron microscope apertures (Fisher Scientific, Pittsburg, PA) were cemented, also were used as apertures. Liquid is ejected from the chamber orifice when a DC voltage is applied across the crystal. A pulse generator (model 214A, Hewlett Packard Corp., Palo Alto, CA) provided a DC voltage signal to the crystal (Fig. 2). Pulse width and amplitude of the generator signal were adjusted so that a pulse to the crystal would produce a single drop.

The maximum drop diameter that could be produced by the crystal was about 1.89 mm. (Maximum displacement of water volume resulting from deformation of the crystal is limited to about 2.5 mm^3.) Larger diameter drops (2.16–3.24 mm) were produced by a solenoid pump (model SV515, Valcor Engineering Corp., Springfield, NJ) (Fig. 1B). Power was supplied to the solenoid pump by a 0–38V Kepco Corp. power supply (model PR-38-5, Kepco Corp., Flushing, NY). The outlet of the pump was machined to a Luer taper to accept Luer-lok needles (Fisher Scientific, Pittsburg, PA). Single, uniform drops were produced by

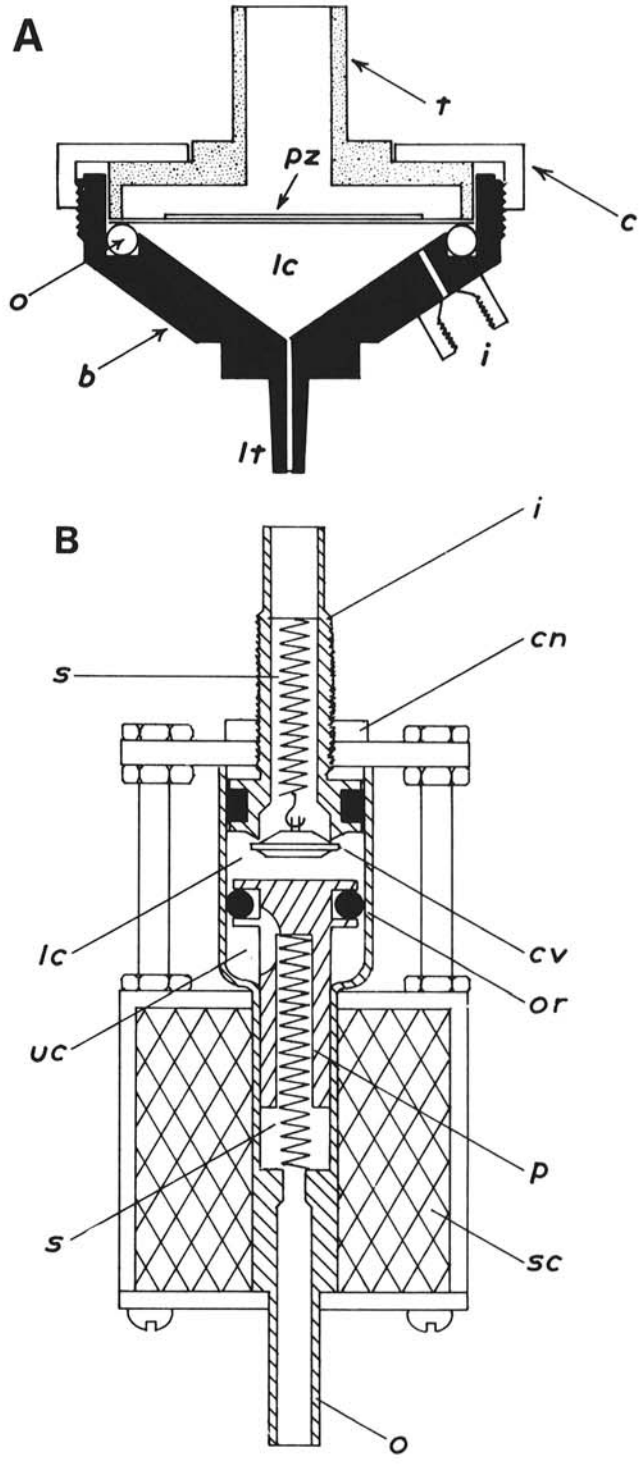

Fig. 1. Schematics of drop-generating devices. **A,** Piezoelectric drop generator. Application of voltage across the piezoelectric crystal (pz), causes the crystal to deform, which produces a downward flexure of the crystal into the liquid chamber (lc) formed by the housing base (b), resulting in the displacement of liquid from the Luer-tapered chamber outlet (lt). Water is supplied to the chamber through the inlet (i). Other components illustrated are: chamber top (t), screw cap (c), and rubber O-ring seal (o). **B,** Solenoid pump drop generator, activated by applying voltage to the solenoid coil (sc), which draws the piston (p) downward against a return spring (s), resulting in the ejection of liquid from the outlet (o). A vacuum-operated check valve (cv) at the top of the lower liquid chamber (lc) opens as the piston moves downward, recharging the lower chamber through the liquid inlet (i). The upper liquid chamber (uc) is recharged as the piston is forced upward by the return spring. The volume of a drop produced by the generator is controlled by voltage amplitude and the combined size of the lower and upper chambers. The latter is adjusted by a checknut (cn) at the top of the generator. Also shown is a rubber O-ring (or) that allows smooth piston operation.

adjusting the power supply voltage and stroke length of the pump.

Photographic system. Voltage signals that were used to activate the drop generators were also applied to a microprocessor-controlled timing circuit (Figs. 2 and 3) to control the firing sequence of one to seven stroboscopic flash units (Fig. 2). Four flash units were used. The voltage signal to the piezoelectric drop generator activated an initial strobe-firing delay mechanism that was controlled by a type 153I-PZ timer (GenRad Corp., Concord, MA). At the end of the primary delay, the microprocessor timing unit fired the four flash units at intervals controlled by the frequency of the oscillator signal (Fig. 2). A photoelectric pick-off unit (model 1536, GenRad Corp., Concord, MA) was used to trigger the primary strobe delay when using the solenoid pump, because the signal emitted by this generator was too variable for accurate strobe timing.

Previous experience with high-speed movies of drop impact indicated that backlighting of the impacting drops was necessary (25). The flash units were mounted together, behind the photographic stage, so that each lamp was 23 cm from a frosted-glass diffusion screen. The diffusion screen was 2.5 cm behind the photographic stage.

All photographs were taken with a Pentax MX 35-mm single-lens reflex camera with the shutter speed set on bulb and the aperture set at f11 or f16 (for magnifications of 2 and 1×, respectively). To achieve magnifications of 1–3× on the film plane, a 50-mm focal-length lens was mounted in reverse position with a reversing ring on a Pentax bellows unit. The film used was Kodak Technical Pan.

Measurement of drop diameters and estimation of drop spread factors on water-sensitive paper. Drops were collected 1 cm below the orifice of each drop generator. Drop diameter was determined microscopically for drops < 2 mm in diameter by catching 20 drops in a two-layer silicone gel preparation (Dow Corning 200 fluid) in a 10-cm-diameter petri dish. The top and bottom gel layers were 100 and 20,000 Cs viscosity, respectively. Microscopic determinations of drop size were completed within 5 min of drop collection to minimize errors resulting from drop dissolution in the silicone gel.

Drops > 2 mm in diameter were collected in a petri dish, then weighed to the nearest milligram and their equivalent diameter (ED) determined from their calculated volume. Drops > 2 mm in diameter do not maintain a strictly spherical shape because of gravitational force acting on their mass (22). ED refers to the diameter of a drop if the drop volume were in fact spherical (22). The definition of ED also is applied to circular areas. Twenty drops were collected in four replicate samples of five drops each. Each sample was collected and weighed in a total time of 20 sec to minimize measurement errors resulting from drop evaporation. To estimate the standard deviation of drop diameter for drops > 2 mm in diameter, the calculated mean ED was determined for the four replicate samples. The standard deviation of the four mean EDs was then used as an estimate of the standard error of mean ED in the expression:

$$SD = \sqrt{n}\, se_{(\bar{x})}, \quad (1)$$

in which SD = standard deviation of drop diameter, $n = 5$ (sample size), and $se_{(\bar{x})}$ = standard error of mean ED.

Drops were collected on water-sensitive paper (WSP) (Spraying Systems Inc., Wheaton, IL) during the same test run in which drops were collected for determination of diameter. The diameters of drop traces left on WSP were determined with an image-

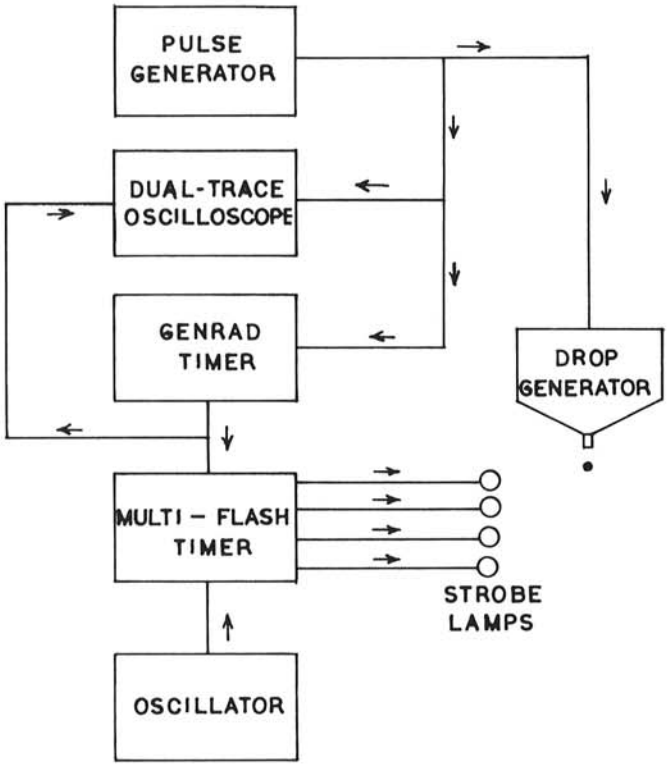

Fig. 2. Schematic of integrated piezoelectric drop generator and microprocessor-controlled strobe timing systems. A 200V amplitude signal from the pulse generator induces a change in the piezoelectric crystal structure, which is housed in the drop generator, resulting in the flexure of the crystal and ejection of a water drop. Signal amplitude and pulse width are monitored on a dual trace oscilloscope. The pulse generator signal is also used to trigger the GenRad (primary) timing device that controls the starting time of a flash sequence. At the end of its timing cycle, the GenRad timer produces a signal that activates the multiflash (secondary) timer that controls the intervals between strobe lamp flashes. The solenoid pump system is similar to the one illustrated, except a constant DC current voltage supply is used in place of the pulse generator. In addition, the signal to the GenRad timer is supplied by a separate photoelectric pick-off unit.

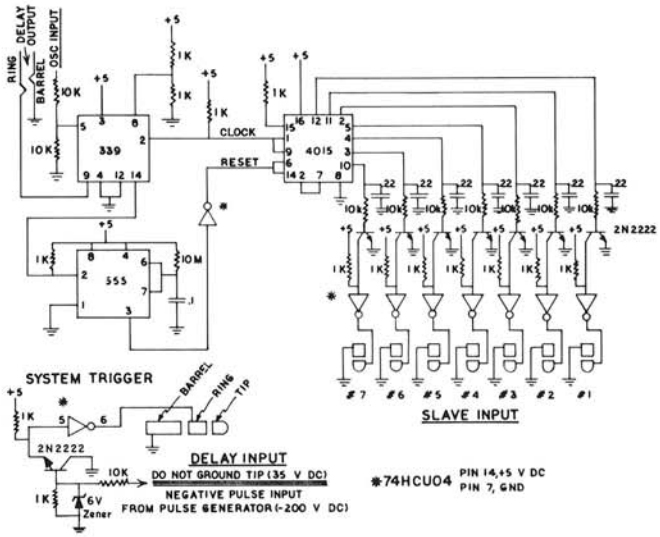

Fig. 3. Diagram of microprocessor-controlled secondary timing circuit used to control the strobe lamp flash interval. The system clock signal is a sine wave generated by an audio oscillator. The oscillator signal is converted to a positive square wave pulse by the first comparator in the IC339 chip. The first comparator continuously transmits the clock signal to the IC4015 static shift register. The 35V incoming GenRad timer signal (DELAY INPUT), which is used to initiate the secondary timing system (see also Fig. 2), is first conditioned as illustrated under SYSTEM TRIGGER, and then input (DELAY OUTPUT) to the second comparator in the IC339 chip via the barrel and ring phone jack connection. When triggered, the IC339 in turn triggers the IC555 monostable vibrator, which transmits a pulse to the IC4015, allowing the IC339 clock signal to sequentially activate the IC4015 static registers at the clock frequency output by the audio oscillator. At activation, each static register outputs a signal that is first conditioned by a 2N2222 transistor and then inverted. The modified signal causes an attached strobe lamp to fire. The IC555 monostable vibrator signal drops to 0V after about 5 sec and resets the IC4015 static registers to 0V. Up to seven strobe lamps can be connected to the system.

analyzing computer (Dapple Systems Inc., Sunnyvale, CA). The computer program reports the area of individual drops from which drop EDs were calculated. For many purposes, it is more efficient to collect, count, and measure large numbers of drops on WSP than in silicone gel preparations. WSP can also be stored for extended periods of time after use.

Estimation of drop velocity. Multiple-exposure photographs were taken of drops at a distance of 6 cm below the orifice of the drop generators. A millimeter scale, included in the photograph, was used to calculate drop velocity, given the microprocessor-controlled time interval between strobe flashes. Two determinations of velocity were made for each drop diameter.

Observed drop velocities at 6 cm below the orifice were compared with theoretical values obtained by assuming an initial velocity of 0 $cm \cdot s^{-1}$ at the orifice. The theoretical relation for velocity at time t (v_t) is:

$$v_t = V_T(1 - e^{-t/\tau}), \quad (2)$$

in which V_T = terminal velocity ($cm \cdot s^{-1}$), t = time (sec), and τ = relaxation time (sec).

Values for V_T were obtained from the relation:

$$V_T = 880.0[1 - \exp(-((d + 0.115)/1.718)^{1.336})], \quad (3)$$

in which d = drop diameter (mm). Equation 3 is an empirical fit to values for V_T calculated from a much more complicated set of theoretical relations given by Beard (2), where nonlinear $R^2 = 0.999$, $P[F(3,46) = 992.6] \leq 0.0001$.

Relaxation time (τ) was calculated as:

$$\tau = 0.2733 + 0.1153 \log(d). \quad (4)$$

Eq. 4 also was an empirical relation developed from experimental values and a theoretical relation for τ given by Pruppacher (23), where $R^2 = 0.992$, $P[F(1,5) = 624.6] \leq 0.0001$).

Time to reach a distance of 6 cm below the orifice was calculated iteratively from the relation:

$$X_t = V_T(t + \tau e^{-t/\tau} - \tau), \quad (5)$$

in which X_t = distance of fall in time t. Note that eq. 5 is just the definite integral of eq. 2. v_t was then calculated by substituting the value for t into eq. 2.

RESULTS

Production of single, uniform drops. A range of drop sizes can be produced with either the piezoelectric drop generator or the solenoid pump drop generator (Table 1). In preliminary tests of the solenoid pump, it was found that this generator could produce single, uniform drops as small as 0.2 mm in diameter. However, production of such small drops was both easier and more reliable with the piezoelectric crystal.

Three phenomena that have been observed with ink-jet printers (18) were also observed with both of our drop generators. First, if the water supply was tap water, mineral deposits built up at the drop generator's orifice and altered the drops' trajectories. Consequently, reliable operation of either drop generator required the use of deionized water to prevent occlusion of the aperture. Second, air pockets in the chamber of either drop generator resulted in the production of nonuniform drops and erratic drop output. However, the formation of air pockets was minimized by selecting generator operating parameters that minimized recoil of the liquid volume from the orifice (Table 1). Third, if the volume of liquid displaced by the generator was too large relative to the size of the aperture, small satellite drops also were produced. Appropriate selection of the generator's operating parameters minimized difficulties in this case as well.

In general, selection of the optimum set of drop generator operating parameters was achieved by trial and error. For the piezoelectric drop generator, production of single, uniform drops was controlled by an appropriate combination of generator aperture diameter, hydraulic head height of the water reservoir, and signal pulse width (Table 1). The effect of variation in generator voltage level could not be examined in this study because voltage level was not adjustable in the range 100–200V.

Drops could not be produced with any of the apertures at the next lowest selectable voltage level of 100V even when hydraulic head height and generator pulse width were set to their maximum levels. For a given aperture diameter, drop diameter could be altered by varying generator pulse width and hydraulic head height of the water reservoir supplying the generator. However, the most reliable drop production was obtained by adjusting head height so that it was just sufficient to hold water in the generator chamber against gravitational flow (Table 1).

System operating parameters given in Table 1 should only be

TABLE 1. Operating parameters of piezoelectric and solenoid pump drop generators required for production of specific drop sizes

Drop diameter (mm)		Generator	Aperture diameter	Voltage amplitude[b]	Pulse width	Head height[c]	Stroke length
Mean	C.V.[d]	type[a]	(mm)	(V)	(msec)	(mm)	(mm)
0.18	2.2	P	0.060 (u)[e]	200	2.30	25	NA[f]
0.24	2.0	P	0.100 (u)	200	1.16	40	NA
0.36	1.3	P	0.254 (n)	200	2.20	69	NA
0.53	1.4	P	0.250 (u)	200	0.96	25	NA
0.65	1.8	P	0.400 (u)	200	1.36	25	NA
0.72	1.1	P	0.305 (n)	200	2.20	59	NA
0.93	0.8	P	0.500 (u)	200	1.80	25	NA
0.95	1.3	P	0.406 (n)	200	3.75	37	NA
1.34	1.6	P	0.584 (n)	200	2.60	27	NA
1.55	4.8	P	0.838 (n)	200	3.50	18	NA
1.89	1.4	P	1.194 (n)	200	3.50	15	NA
2.16	3.6	S	1.194 (n)	32.2	NA	NA	8.64
3.24	0.8	S	1.194 (u)	23.5	NA	NA	7.34

[a] P = piezoelectric crystal, S = solenoid pump.
[b] DC voltage signal for piezoelectric crystal was a pulse with adjustable width, whereas the solenoid pump received a continuous pulse width of about 100–150 msec.
[c] Height of reservoir above generator aperture.
[d] C.V. = coefficient of variation.
[e] n = Aperture was a needle that had been cut off to a length of 8 mm, u = aperture was an uncut needle.
[f] NA indicates not applicable.

regarded as approximate. Drop size also was found to vary slightly with change in O-ring pressure on the piezoelectric disk produced by screwing the generator cap to different torque specifications. Rather than quantifying cap torque, we found that for a fixed head height, pulse width could be adjusted so that it was possible to reproduce drop sizes between experimental setups with an error of no more than 5%.

The solenoid pump contained a check-valve that ensured positive displacement of the liquid volume in the chamber (Fig. 1B). Therefore, control of the hydraulic head of the water reservoir was not necessary. In this system, drop size was controlled by piston stroke length, aperture diameter, and DC voltage (Table 1).

Measurement of drop diameters and estimation of drop spread factors on WSP. The estimated coefficient of variation (C.V.) for each drop diameter produced by either the piezoelectric or solenoid pump drop generator was so small that all drops were considered uniform in size (Table 1). Although only four replicate samples of five drops were used to estimate mean diameter for drops produced by the solenoid pump generator, the estimated C.V.s for these drops are comparable to those for the piezoelectric generator (Table 1), indicating that the sample size used to estimate drop diameter by weighing was quite adequate.

A significant linear relationship between diameter of the drop trace on WSP and original drop diameter was obtained with linear regression analysis (Fig. 4). The model accounted for 99% of experimental variation: $P[F(1,222) = 15{,}269] \leq 0.0001$. An analysis performed previously on 178 preliminary observations yielded an almost identical model to the one presented (Fig. 4).

Estimation of drop velocity. Drop velocities measured at 6 cm below the drop generator orifice agreed well with predicted velocities (Table 2). Observed velocities for drops ≥ 0.654 mm in diameter slightly exceeded predicted values, so initial velocity must be nonzero for these drops. In contrast, drops with diameters < 0.654 mm had observed velocities slightly lower than predicted values. Reichard et al (25) have observed that the process of drop release involves the formation of a liquid ligament. Release occurs when the ligament is broken. Surface tension forces, acting during this process, have been observed to impart a small acceleration in the positive vertical direction (Reichard, *unpublished*).

Drop impact on a surface. Drops 1.8 mm in diameter were produced by the piezoelectric drop generator and allowed to impact on an immature strawberry fruit (*Fragaria* × *ananassa*). Single drops were released from a height of 50 cm. Drops were aimed at the fruit so that the point of impact on the fruit surface would lie in a vertical plane that bisected the fruit and that was parallel to the film plane. The primary flash unit delay was visually determined. All photographs were taken with a 2 msec strobe flash interval (Fig. 5). The primary delay was initially set to record two exposures of incident drop travel just before drop impact on the fruit surface (Fig. 5A). An early stage in the production of the splash droplets can also be seen. The velocity of drop impact, as determined from the photographic record of drop travel, was estimated to be 273.9 $cm \cdot s^{-1}$ (Fig. 5A).

The effects of incident drop diameter, velocity, and angle of impact on the number, diameters, and velocities of splash droplets produced are readily determined with high-speed still photography. An example of splash droplet production after impact of a 1.8-mm-diameter drop falling from a height of 50 cm is given in Figure 5B. Two pairs of droplets were specifically identified for which diameter and velocity could be measured. However, at least five such droplet pairs can be seen (Fig. 5B).

The angle of drop impact on the fruit surface (*a*) can be defined as the angle between the trajectory of the incident drop (*i*) and the vector (*n*), which is normal to the tangent vector (*t*) at the point of drop impact (Fig. 5B). The mean angle of droplet flight (*b*) along trajectory *o* can also be defined relative to the normal vector, *n* (Fig. 5B). Defining the incident drop trajectory and the mean droplet takeoff trajectory in this manner conveniently relates the mean droplet trajectory to the vector that is tangent to the point of incident drop impact.

TABLE 2. Drop velocity at 6 cm below the drop generator aperture

Drop diameter (mm)	Observed drop velocity ($cm \cdot s^{-1}$)	Predicted drop velocity[a] ($cm \cdot s^{-1}$)
0.24	85.5	72.3
0.53	104.7	92.7
0.65	102.3	99.6
0.73	96.8	103.2
0.93	103.1	112.0
0.95	95.7	112.7
1.34	106.7	124.9
1.55	76.3	129.7
1.89	103.7	135.4
2.16	116.5	138.7
3.25	156.3	144.0

[a] Based on equations 2 and 5 in text.

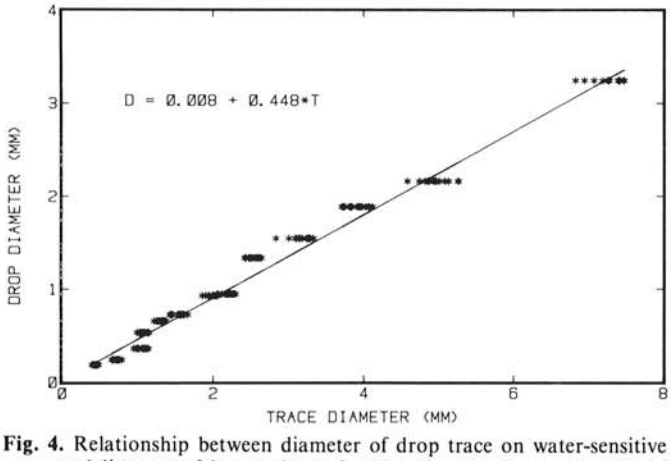

Fig. 4. Relationship between diameter of drop trace on water-sensitive paper and diameter of drop as determined by microscopic measurement of drops in silicone gel (< 2 mm diameter) or weighing 20 drops collected in a petri dish (> 2 mm diameter).

DISCUSSION

The drop-generating and photographic system that has been developed allows detailed examination of phenomena associated with the impact of raindrops or drips from the plant canopy. High-speed cinematography has frequently been employed for studying drop impact events (15,16,20). However, the size, number, and velocity of droplets produced by a splash impact can be easily recorded with our methods at a small fraction of the cost entailed in cinematographic methods. Furthermore, the analysis of drop sizes produced by either the piezoelectric or solenoid pump drop generators demonstrated that drops in the range of 0.18–3.24 mm diameter can be produced with acceptable uniformity (Table 1).

Fitt et al (8) provided a thorough discussion of methods previously employed for determining the size and distribution of splash droplets. Among the methods described is the use of fixed photographic film for determining size and distribution of droplets (5). Our tests show that WSP can also be used for assessing the distribution of splash droplets (Fig. 4). A disadvantage of using WSP, as opposed to fixed photographic film, is that propagule numbers within droplets cannot be determined simultaneously. However, use of WSP offers the advantage of speed in analysis of droplet distributions when used in conjunction with computer image analysis.

Large drops are probably important in splash droplet production because of their high kinetic energy (10,24,26). The solenoid pump used in our drop-generating system can produce

drops up to 3.24 mm in diameter (Table 1). Drops formed by canopy drip may be up to 6 or 7 mm in diameter (24). However, pumps with sufficient displacement to produce drops up to 7 mm in diameter are also available. It is also important to be able to study splash events that simulate impacts produced from canopy drip. Our data on initial drop velocities demonstrate that our drop generators are suitable for studying such events (Table 2).

Because a bellows unit was used on the camera, the photographic depth of field was extremely narrow (0.71–3.23 mm for magnifications of 3 down to 1×, respectively). At 1×, we have found that the depth of field is sufficient for accurate determination of droplet number and size (Fig. 5). However, takeoff velocities can only be measured for droplets whose trajectories are parallel to the film plane because of the loss of information that results from projecting a three-dimensional image onto a plane. As a result, multiple photographs will be required to obtain sufficient data to accurately estimate takeoff velocity for a given incident drop size and velocity. The cost of data acquisition using high-speed cinematography would be substantial. For comparison, we estimate that data acquisition costs can be reduced by 95% using the systems described.

The drop production and photographic systems that have been described provide the ability to observe splash events in detail and allow measurement of the size and number of droplets produced as well as their takeoff velocities. Availability of such information, together with observations on resulting droplet distributions, can be used to develop and validate explanatory models of observed distributions of splash-dispersed inoculum. We are currently using these procedures to study the dispersal of *Phytophthora cactorum*, which was previously shown to be splash-dispersed from infected strawberry fruit (13).

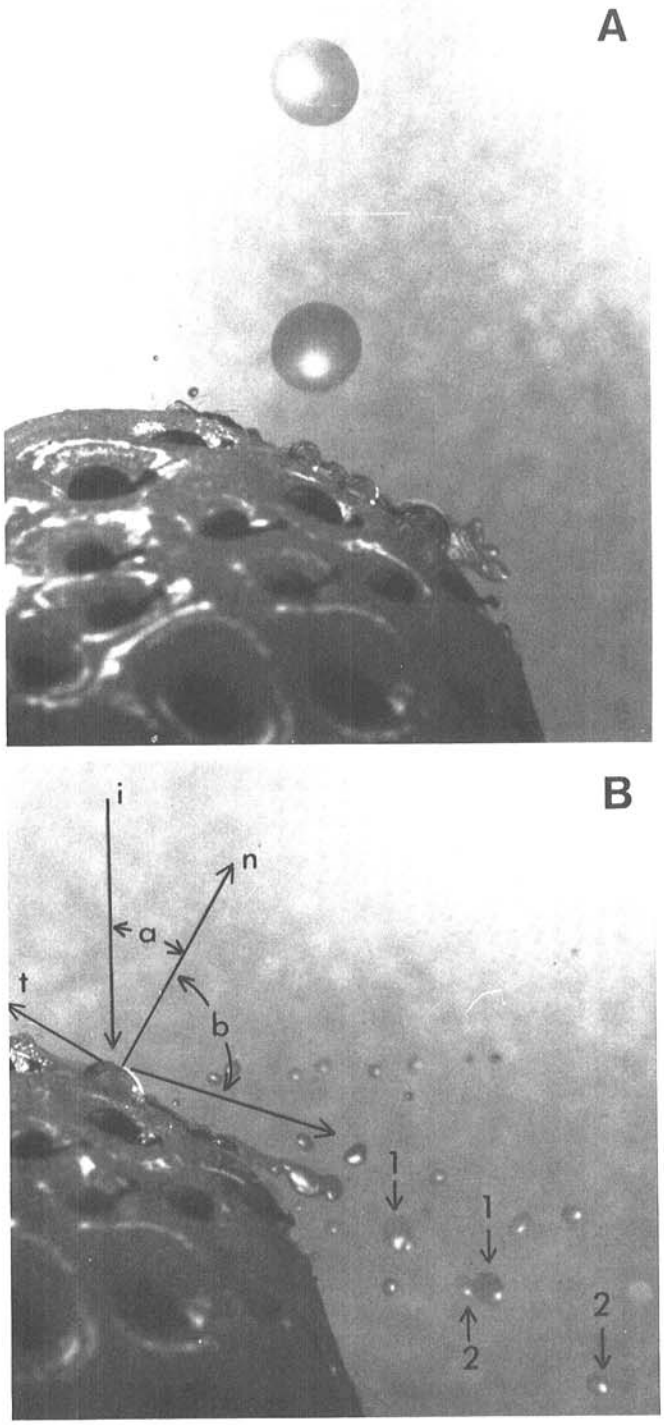

Fig. 5. Production of splash droplets after impact of a 1.8-mm-diameter drop on an immature strawberry fruit. Single drops were released from a height of 50 cm. Flash intervals were 2 msec. **A,** Incident drop just before impact with fruit surface. **B,** Formation of splash droplets after drop impact with fruit surface. Two drops (1 and 2) are shown from which diameter and velocity can be determined. Also shown are vectors for incident drop trajectory (i), the tangent to the surface at the point of impact (t), the vector, n, that is normal to t, and the mean trajectory of the splash droplets. Angles a and b indicate the departures of i and o from n, respectively.

LITERATURE CITED

1. Anonymous. 1985. Piezoelectric Technology: Data for Designers. Vernitron Piezoelectric Div., Bedford, OH. 40 pp.
2. Beard, K. V. 1976. Terminal velocity and shape of cloud and precipitation drops aloft. J. Atmos. Sci. 33:851-864.
3. Best, A. C. 1950. The size distribution of rain drops. Q. J. R. Meteorol. Soc. 76:16-36.
4. Faulwetter, R. F. 1917. Dissemination of angular leafspot of cotton. J. Agric. Res. 8:457-475.
5. Faulwetter, R. F. 1917. Wind-blown rain, a factor in disease dissemination. J. Agric. Res. 10:639-648.
6. Fitt, B. D. L., Lapwood, D. H., and Dancer, S. J. 1983. Dispersal of *Erwinia carotovora* subsp. *atroseptica* in splash droplets. Potato Res. 26:123-131.
7. Fitt, B. D. L., and Lysandrou, M. 1984. Studies on mechanisms of splash dispersal of spores, using *Pseudocercosporella herpotrichoides* spores. Phytopathol. Z. 111:323-331.
8. Fitt, B. D. L., Lysandrou, M., and Turner, R. H. 1982. Measurement of spore-carrying droplets using photographic film and an image-analyzing computer. Plant Pathol. 31:19-24.
9. Fitt, B. D. L., and Nijman, D. J. 1983. Quantitative studies on dispersal of *Pseudocercosporella herpotrichoides* spores from infected wheat straw by simulated rain. Neth. J. Plant. Pathol. 89:198-202.
10. Gregory, P. H. 1970. Microbiology of the Atmosphere. Leonard Hill Publishing, Aylesbury, Bucks, England. 377 pp.
11. Gregory, P. H., Guthrie, E. J., and Bunce, M. 1959. Experiments on splash dispersal of fungus spores. J. Gen. Microbiol. 20:328-354.
12. Griffiths, E., and Hann, C. A. 1976. Dispersal of *Septoria nodorum* spores and spread of glume blotch of wheat in the field. Trans. Br. Mycol. Soc. 67:413-418.
13. Grove, G. G., Madden, L. V., and Ellis, M. A. 1985. Splash dispersal of *Phytophthora cactorum* from infected strawberry fruit. Phytopathology 75:611-615.
14. Gunn, R., and Kinzer, G. D. 1949. The terminal velocity of fall for water droplets in stagnant air. J. Meteorol. 6:243-248.
15. Hobbs, P. V., and Kezweeny, A. J. 1966. Splashing of a water drop. Science 155:1184-1186.
16. Hobbs, P. V., and Osheroff, T. 1967. Splashing of drops on shallow liquids. Science 156:1184-1186.
17. Hunter , J. E., and Kunimoto, R. K. 1974. Dispersal of *Phytophthora palmivora* by wind-blown rain. Phytopathology 64:202-206.
18. Johnson, T. E., and Bower, K. W. 1979. Review of the drop on-demand ink jet with primary emphasis on the Gould jet concept. J. Appl. Photog. Eng. 5:174-178.
19. Laws, J. O., and Parsons, D. A. 1943. The relation of raindrop size to intensity. Trans. Am. Geophys. Union 24:452-460.
20. Macklin, W. C., and Hobbs, P. V. 1969. Subsurface phenomena and the splashing of drops on shallow liquids. Science 166:107-108.

21. Marshall, J. S., and Palmer, W. M. 1948. The tribution of raindrops with size. J. Meteorol. 5:165-166.
22. Pruppacher, H. R., and Klett, J. D. 1980. Microphysics of clouds and precipitation. Reidel Publishing, London. 714 pp.
23. Qian, S.-X., Snow, J. B., Tzeng, H.-M., and Chang, R. K. 1986. Lasing droplets: Highlighting the liquid-air interface by laser emission. Science 231:486-488.
24. Quinn, N. W., and Laflen, J. M. 1983. Characteristics of raindrop throughfall under corn canopy. Trans. Am. Soc. Agric. Eng. 26:1445-1450.
25. Reichard, D. L., Brazee, R. D., Bukovac, M. J., and Fox, R. D. 1986. A system for studying impaction on leaf surfaces. Trans. Am. Soc. Agric. Eng. 29:(In press).
26. Saville, D. B. O., and Hayhoe, H. N. 1978. The potential effect of drop size on efficiency of splash-cup and springboard dispersal devices. Can. J. Bot. 56:127-128.
27. Schub, R. L. 1983. Epidemiology of *Phytophthora capsici* on bell pepper. J. Agric. Sci. 100:7-11.
28. Stedman, O. J. 1979. Patterns of unobstructed splash dispersal. Ann. Appl. Biol. 91:271-285.
29. Stedman, O. J. 1980. Splash droplet and spore dispersal studies in field beans (*Vicia faba* L.). Agric. Meteorol. 21:111-127.
30. Stepanov, K. M. 1935. Dissemination of infective diseases of plants by air current. Tr. Zashch. Rast. Ser. 2. 8:1-68. (In Russian)
31. von Nageli, C. 1877. Die Niederen Pilze. Oldenburg, Munich. 285 pp.
32. Young, B. W. 1984. A device for the controlled production and placement of individual droplets. ASTM Symp. Pestic. Formulation Appl. Systems 5th. Kansas City.